Chemical Geology 401 (2015) 140–150

Contents lists available at ScienceDirect

Chemical Geology

journal homepage: www.elsevier.com/locate/chemgeo

Lead concentrations and isotope ratios in speleothems as proxies for atmospheric metal pollution since the industrial revolution

Mohammed Allan [a,*], Nathalie Fagel [a], Maité Van Rampelbergh [b], James Baldini [c], Jean Riotte [d], Hai Cheng [e], R. Lawrence Edwards [e], David Gillikin [f], Yves Quinif [g], Sophie Verheyden [b,h]

[a] AGEs, Département de Géologie, Université de Liège, Allée du 6 Août, B18, Sart Tilman B-4000, Liège, Belgium
[b] Earth System Sciences Department, Vrije Universiteit Brussel (VUB), Pleinlaan 2, B-1050 Brussels, Belgium
[c] Department of Earth Sciences, Durham University, Durham DH1 3LE, UK
[d] Géosciences Environnement Toulouse (GET), UPS, IRD, CNRS, 31400 Toulouse, France
[e] Department of of Earth Sciences, University of Minnesota, 310 Pillsbury Drive, SE, Minneapolis, MN 55455, USA
[f] Department of Geology, Union College, 807 Union St, Schenectady, NY, USA
[g] Faculté Polytechnique, Université de Mons. Rue de Houdain 9, 7000 Mons, Belgium
[h] Earth and History of Life, Royal Belgian Institute of Natural Sciences, Jennerstreet 13, 1000 Brussels, Belgium

ARTICLE INFO

Article history:
Received 15 May 2014
Received in revised form 23 February 2015
Accepted 24 February 2015
Available online 5 March 2015

Edited by: Prof. L. Reisberg

Keywords:
Atmospheric pollution
Trace metals
Pb isotopes
Stalagmites
Western Europe

ABSTRACT

Lead concentrations and isotope ratios from two speleothems from the Han-sur-Lesse cave in southern Belgium were measured in order to study the ability of speleothems to act as archives of atmospheric pollution. To address this aim we analyzed trace elemental Al and Pb compositions by LA-ICP-MS and ICP-MS as well as Pb isotopes by MC-ICP-MS. The results help to identify three intervals characterized by particularly high enrichment of Pb: from 1880 to 1905 AD, from 1945 to 1965 AD, and from 1975 to 1990 AD. The speleothem record shows similar changes as the known historical atmospheric pollution level in Belgium. Lead isotope ratios discriminate between Pb sources and confirm that coal and gasoline combustion, combined with regional metallurgical activities, were the predominant Pb pollution sources in the stalagmites during the last 250 years. This study opens possibilities to determine anthropogenic versus natural metal sources in well-dated speleothem archives.

1. Introduction

The increase in atmospheric metal deposition compared to prehistoric levels is particularly marked in Europe since at least 2000 years. Mining and metallurgical activities, and later coal burning and transport emissions were the principal anthropogenic sources (Nriagu, 1979; Pacyna and Pacyna, 2001; Pacyna et al., 2007). Belgium, as part of the northwestern European industrial basin, has a long industrial history. To assess the extent of atmospheric contamination, it is necessary to identify the main past and present sources of trace metal emissions. The isotopic ratios of Pb ($^{208}Pb/^{206}Pb$ and $^{206}Pb/^{207}Pb$) are used in environmental deposits to quantify anthropogenic Pb inputs compared to the natural/local background and to trace Pb emission sources (e.g., Geagea et al., 2008). Atmospheric metal pollution is directly recorded by several types of environmental archives such as lake sediments (e.g., Shirahata et al., 1980; Brännvall et al., 1999; Outridge et al., 2011), marine deposits (e.g., Gobeil et al., 1999), ice (e.g., Boutron et al., 1991, 1994; Hong et al., 1994; Rosman et al., 1997), soils (e.g., Elless and Lee, 1998) and peat (e.g., Shotyk et al., 2005; Allan et al., 2013). However, some areas with abundant past heavy metal pollution lack suitable archives due to dating uncertainties and limited spatial occurrence of some of these archives (e.g., ice). The abundance of speleothems (and stalagmites in particular) and their precise dating possibilities suggest that they might make ideal archives for the reconstruction of historical metal pollution fluxes. During the last decades, speleothem studies have enhanced our knowledge of continental climate and environment, in particular the precise chronology of past decadal to millennial climate and environmental changes up to 600 ka, limit of the U/Th dating method (Genty et al., 2003; Wang et al. 2008; Drysdale et al., 2009; Fleitmann et al., 2012). Their amenability to radiometric dating using the U-series, mainly the U/Th method (Li et al., 1989; Hellstrom et al., 1998; Kaufman et al., 1998) with a precision of better than 0.5%, combined with layer counting (e.g., McMillan et al., 2005, Genty et al., 2006; Verheyden et al., 2006) in seasonally layered speleothems offer a high resolution archive for reconstructions of past climate and environment (e.g., Fairchild and Baker, 2012). Until now, the potential of speleothems

* Corresponding author. Tel.: +32 4 366 98 71; fax: +32 4 366 20 29.
E-mail addresses: mouhamdallan@hotmail.fr, mallan@doct.ulg.ac.be (M. Allan).

http://dx.doi.org/10.1016/j.chemgeo.2015.02.035
0009-2541/

for recording environmental pollution is largely unexplored and mainly focused on quantifying aerosol contributions in touristic caves (Chang et al., 2008; Dredge et al., 2013).

The goal of this study is to define the high Pb concentrations and Pb content variability in the upper 250 years of two northwest European speleothems. We verify the reproducibility of the Pb time-series in and between speleothems. We discuss possible drivers for the increased Pb concentration and investigate the eventual link with known anthropogenic atmospheric Pb pollution. The study therefore assesses the ability of speleothems to register past atmospheric metal fall-outs despite the transfer of the signal through the soil and the host rock. To address this aim we analyzed speleothem Pb and Al compositions by LA-ICP-MS and ICP-MS as well as Pb isotope ratios by MC-ICP-MS. The elemental and isotopic Pb signature in speleothems is compared with that of other records from the same area to establish a potential link with the historical atmospheric pollution.

1.1. State of the art

Speleothems such as stalagmites and flowstones are increasingly used for paleoclimatic research. They contain several already well-studied climate and environmental proxies (Fairchild and Baker, 2012). The oxygen isotopic composition of speleothems in tropical areas varies with changes in the monsoon intensity through changes in the contribution of summer monsoon (e.g., Wang et al., 2008; Scholte and De Geest, 2010). In northern latitudes the $\delta^{18}O$ seems influenced by temperature as well as rainfall amount (Mangini et al., 2005; Mattey et al., 2008). The spatial variability of the $\delta^{18}O$ signature of speleothems was proven to reflect the regional air circulation patterns in Europe (McDermott et al., 2011). The $\delta^{13}C$ in speleothems from regions in which most types of vegetation employ the same photosynthetic pathway, as in Europe, mainly reflects changes in the intensity of vegetation cover or soil bacterial activity (Genty and Massault, 1999). The relative contribution of isotopically light carbon from the soil compared to that of the host limestone increases in warm periods. Genty et al. (2003) demonstrated that the $\delta^{13}C$ changes recorded in the Villars speleothems from France are the equivalent of the Dansgaard–Oeschger cycles identified in polar ice cores. In addition to stable isotope ratios, speleothem trace element (e.g., Mg, Ba, Sr, U) compositions represent a large proportion of the studied speleothem proxies. These elements seem to be influenced by the vadose hydrology in the epikarst zone above the drip-water site. Therefore they may give information on the paleo-recharge amounts, i.e. balance of precipitation and evaporation, in speleothems (Baker et al., 1997; Fairchild et al., 2001). Variations in trace element concentration in stalagmites depend on: 1) chemical mobilization of elements in the soil (Blaser et al., 2000; Jo et al., 2010; 2) contributions from the surrounding limestone; 3) dry deposition of dust or tephra deposition at the surface (Dredge et al., 2013; 4) the nature of the transport from the soil zone through the host rock to the cave environment and 5) carbonate precipitation conditions (Fairchild and Treble, 2009; Fairchild et al., 2010; Jo et al., 2010; Hartland et al., 2011; Wynn et al., 2014). Little research has studied the transmission of Pb from soil to cave (e.g., Borsato et al., 2007; Baldini et al., 2012; Hartland et al., 2012). Hartland et al. (2012) showed that the Pb mobilization in forest soils overlying limestone may be strongly related to the presence of organic matter (colloidal transportation). They further suggested that the transportation by organic colloids should be indicated by covariation of elements that are strongly bound to colloids (such as Pb, Al). Borsato et al. (2007) suggested that the transport of Pb can be attributed to a combination of the effects of mobile organic matter and high flow from the soil to the speleothem. Recently, uranium (Siklosy et al., 2011), anthropogenic sulfate (Frisia et al., 2005; Wynn et al., 2008), and lead (McFarlane et al., 2013) were detected in speleothems in a specific context of pollution demonstrating their potential as archives for human impact on the environment. Wynn et al. (2010) and Frisia et al. (2005) showed that the sulfate in speleothem calcite is indicative of atmospheric pollution opening the possibility of speleothems to be archives of atmospheric pollution.

2. Material and methods

Two speleothems from the Han-sur-Lesse cave system developing in Givetian (Devonian) limestone and located in southern Belgium (Quinif and Bastin, 1986) are investigated (Fig. 1). Because the area is part of the natural reserve of Han, the area was not impacted by anthropogenic pollution, other than that derived from the atmosphere. The surface runoff over the cave system is close to zero (Bonniver, 2011) indicating that most of the natural rainfall infiltrates into the soil toward the vadose zone after some evapotranspiration, particularly during spring and summer. This percolation water feeds the speleothems in the cave.

The Proserpine stalagmite is a 2 meter long and ~1 m large stalagmite located in the Salle du Dôme in the touristic part of the Han-sur-Lesse cave system. Two cores were collected in 2011 (S1) and 2001 (S2) and used for this study. The Proserpine stalagmite is layered (two layers per year) over the last 500 years. A detailed study of the stalagmite, based on the S2 core is found in Verheyden et al. (2006). The chronology of the speleothem and thus of the cores is based on U-series dating, combined with layer counting and on ^{14}C dating of the straw incorporated in the stalagmite (Fig. 2) (Verheyden et al., 2006; Van Rampelbergh et al., 2014). Layer counting was carried out on high-resolution scans using Adobe Photoshop and by using a microscope. In 2011 the S1 core was taken at ~50 cm from the S2 core and presented a similar sedimentological pattern. The upper 13 cm from stalagmite core S1 and the upper 10 cm from core S2, are presented in this paper (Fig. 2). According to previous studies, a hiatus of at least 83 years occurred from ~1870 to 1790 AD which corresponds to a sedimentological perturbation at ~9 cm from the top of the stalagmite when core S2 was sampled in 2001 (Verheyden et al., 2006). The calcite deposition at this level is heavily disturbed with straw pieces embedded in the calcite (Verheyden et al., 2006). The straw pieces are interpreted to be relics of torches used in the cave or even from fires lit on the paleo-surface of the stalagmite to illuminate the Salle-du-Dôme chamber (Verheyden et al., 2006). The cave has been visited since 1700 AD as indicated by first perturbations in the stalagmite (Verheyden et al., 2006).

In addition to the Proserpine stalagmite cores, we present Pb concentration data from 'La Timide' stalagmite (S3), a 35.5 centimeter-long candle-shaped stalagmite. The stalagmite was sampled in 2004 in the 'Réseau Renversé', a non-touristic part of the Han-sur-Lesse cave located more than 200 m from the entrance beyond a siphon that was by-passed by a tunnel opened in 1961 AD. The stalagmite was therefore totally preserved from direct aerosol deposition until recently. The upper 3.5 cm, corresponding to the last 250 years, is presented in this paper (Fig. 2).

U-series dating was performed on an ICP-MS Finnigan ELEMENT mass spectrometer at the University of Minnesota (USA) for cores S2 (Verheyden et al., 2006) and S3 (this paper) and using a Thermo NEPTUNE MC-ICP-MS at the Laboratoire Géosciences et Environnement, Toulouse (GET) for S1 (this paper). Uranium and thorium chemical separation and purification procedures are described in Edwards et al. (1987) and Cheng et al. (2009a, 2009b). All ages are reported as years AD (Table 1).

The three stalagmites (S1, S2 and S3) were measured with different resolution and by somewhat different methods. For S1, Al and Pb concentrations were determined using a Thermo XSeries2 ICP-MS with an ESI New Wave UP-193FX Fast ExcimerArF laser of 193 nm at the Royal Museum for Central Africa (Tervuren, Belgium). Spots were made of 50 μm diameter (spaced at 500–1000 μm intervals) (n = 205). For S1, the upper 4 cm were duplicated by continuous ablation with a scan speed of 10–30 μm s^{-1} with 22 μm intervals between two measurements (Fig. 2). Total Al and Pb blanks were negligible and ranged from 0.0009 μg g^{-1} (for Pb) to 0.04 μg g^{-1} (for Al). Both Al and Pb blanks were below their limit of detection (0.01 μg g^{-1} for Pb and 0.2 μg g^{-1}

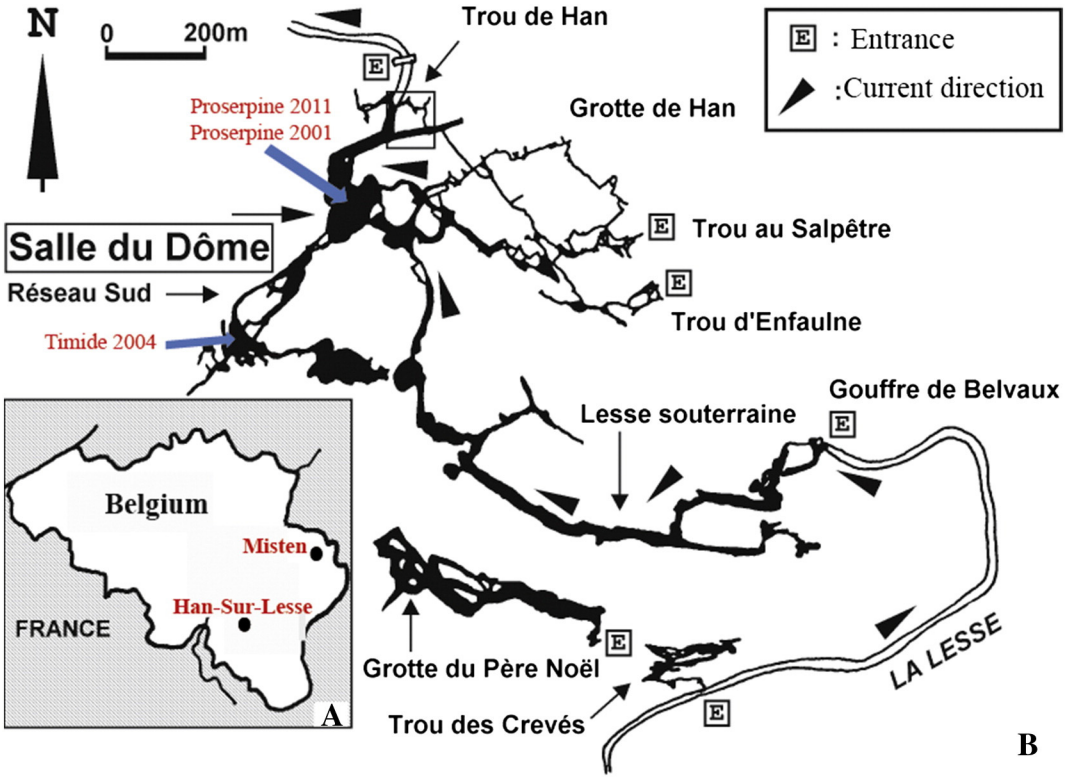

Fig. 1. A—Map of Belgium, displaying sample sites (black dot) for Han-sur-Lesse cave and Misten peat bog. B—Map of the Han-sur-Lesse cave system, from which Proserpine 2010 (S1), Proserpine 2001 (S2) and La Timide (S3) stalagmite cores were collected.

for Al) representing usually less than 0.1% of average sample concentrations.

Seventy-five sample powders were obtained from core S2, by microdrilling using a 700-micron tungsten carbide drill bit at 1.200 micron mean spatial resolution. The powders were dissolved in nitric acid and Al and Pb concentrations determined using a Thermo XSeries2 ICP-MS in the Department of Earth Sciences, Durham University (Durham, UK).

For S3, concentrations (n = 140) were measured by LA-ICP-MS (CETAC LSX-213) at Union College, Schenectady (NY, USA). Spots of 50 μm diameter were made spaced at 250 μm intervals. Blank concentrations represent usually less than 0.0008 μg g^{-1} for Pb and <0.03 μg g^{-1} for Al and therefore are considered negligible. The limits of quantification were calculated from the intensity and standard deviation measurements of 20 blanks. For all stalagmite cores, with each series of samples, four certified reference materials (NIST 610, NIST 612, MACS-1, and MACS-3) were analyzed in order to determine the precision and accuracy of analytical procedures. Comparison between reference values and measured values shows that the reproducibility was satisfactory (more than 70%). Calcium was used as internal standard and assumed to be 40% of the rather pure speleothem $CaCO_3$. The different spatial resolutions handled and slight lateral variations in the Proserpine stalagmite may explain observed differences in metal concentrations between both cores S1 and S2.

Lead isotope ratios were determined in core S1 (Table. 2). After cleaning of the speleothem surface with ethanol and HCl, dried calcite samples (200–400 mg taken by a micro-drill) were dissolved in HNO_3 at 125 °C for 48 h. After evaporation, 2 ml of 6 M HCl were added to ensure complete digestion and the solutions were evaporated. The Pb fraction was extracted after sample dissolution in 0.8 M HBr using AG1-X8 resin in a Teflon column (Weis et al., 2005). Lead isotopic ratios were measured by a Nu Instruments MC-ICP-MS at the Department of Earth and Environment Sciences (Université Libre de Bruxelles, Belgium). Total procedural Pb blanks were ≤0.4 ng and considered as negligible relative to Pb contents in the individual samples (Pb content >40 ng). Mass fractionation for Pb was corrected by using Tl as an internal standard. NBS981 standard was repeatedly measured in alternation with samples to correct for instrumental drift. The isotope ratios of the NBS981 standard were stable during the analysis session [n = 50, $^{208}Pb/^{204}Pb = 36.6998 \pm 0.0027$ (2 σ), $^{207}Pb/^{204}Pb = 15.4930 \pm 0.0010$ (2 σ), $^{206}Pb/^{204}Pb = 16.9376 \pm 0.0010$ (2 σ)]. The Pb isotope ratios of standard measurements are consistent with the recommended values and are in agreement with the laboratory long term values ($^{208}Pb/^{204}Pb = 36.7156 \pm 0.089$, $^{207}Pb/^{204}Pb = 15.4970 \pm 0.0066$, $^{206}Pb/^{204}Pb = 16.9405 \pm 0.0037$, n = 1630). Mass fractionation for Pb was corrected by using Tl as an internal standard.

3. Results

3.1. Chronology

The chronology of the Proserpine stalagmite is well established (Verheyden et al., 2006; Van Rampelbergh et al., 2014). Based on the seasonal layering with deposition of one dark and one light layer every year in the stalagmite we can easily count back the layers from the surface to the sedimentological perturbation at ~10 cm from the top where straw was found in the stalagmite. For S1, counting back from the upper layer (end 2010 AD), 145 ± 3 layer alternations are visible corresponding to the period from 1870 to 2010 (~upper 10 cm). The number of years obtained by layer counting is then compared with the number of years suggested by U/Th dates. For S2, the age was constructed based on layer counting, U/Th dates and one ^{14}C date (Verheyden et al., 2006). Layer counting from the top (2001 AD) down to ~9 cm (133 ± 10 layer couples) places the restart of layering at 1870 AD above the perturbation (Fig. 2). The growth rate in S1 and S2 is commonly 1 mm/year. The upper 230 years (~10 cm) of Proserpine stalagmite consist of grayish calcite (Fig. 2) because of the incorporation of black carbon from torches and graphite lamps used until 2001

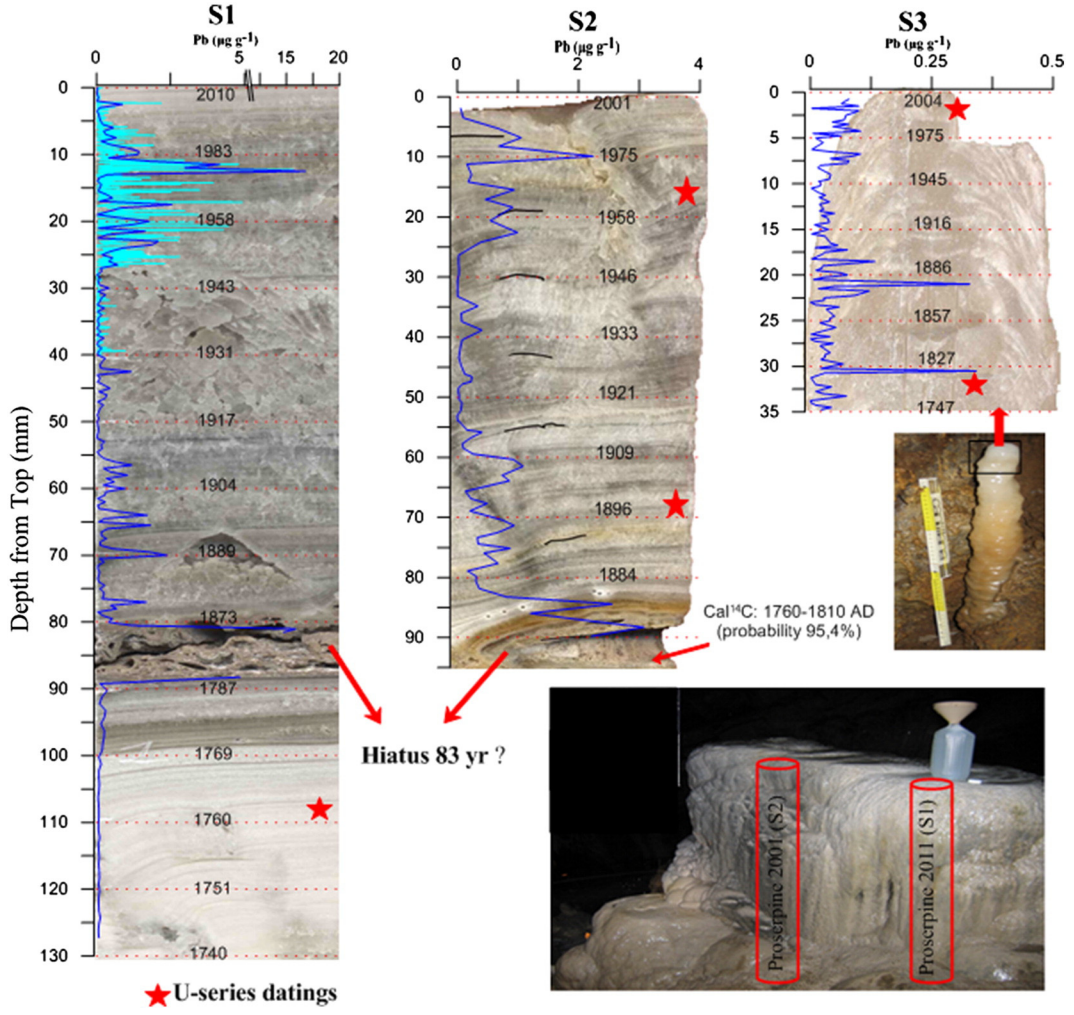

Fig. 2. Profiles of Pb (dark blue curve; in µg g^{-1}) vs core depth (in mm) measured in three stalagmite cores (S1, S2 from the Proserpine stalagmite and S3 from the La Timide stalagmite). Light blue color corresponds to the upper 4 cm of the S1 core, for which Pb concentrations were measured by LA-ICP-MS operated in continuous mode with a scan speed of 10–30 µm s^{-1} with 22 µm intervals between measurements. The red stars represent the levels which have been dated by U series techniques. Straw found in core S2 at the level corresponding to a sedimentary hiatus was dated by ^{14}C.

in this touristic part of the cave. The U/Th results of the S2 core not yet published are given in Table 1.

Table 1 gives the U/Th dating results for the candle shaped Timide stalagmite (S3). Based on the ages and height of the samples that were dated, we can calculate average growth rate in mm/year. The average growth rate varies throughout the core ranging from 0.03 to 0.17 mm/year. The average growth rate in the Timide stalagmite is notably highest (0.17 mm/year) since ~1815 AD. The age model resolution in this stalagmite (S3) is less good than those in S1 and S2 because there are no visible laminae and it is not possible to count them. However, the stalagmite was incorporated in this paper because a change in Pb content similar to that seen in cores S1 and S2 was observed, despite the fact that S3 was collected from another part of the cave.

3.2. Pb and Al concentrations

Lead concentrations of S1 range between 0.01 and 17 µg g^{-1}, between 0.007 and 3 µg g^{-1} for S2 and between 0.001 and 0.4 µg g^{-1} for S3 (Fig. 2, see supplementary data). The Pb content of core S3 is ~ten times less than that of S1 and S2. Both analytical techniques used for Pb measurements in speleothem cores S1 (LA-ICP-MS) and S2 (ICP-MS) produced very similar results. The reproducibility of the Pb curve in Proserpine stalagmite cores S1 and S2, although measured with different methods and in different cores, demonstrates the robustness of the lead signal in speleothems. At approximately 1820 AD, increased Pb concentrations were detected in S3 but cannot be visible in S1 and S2 because a growth hiatus of at least 83 years occurred from 1790 to 1870 AD in the Proserpine stalagmite. Mean Pb concentrations since 1870 AD are more than twice than those observed before 1780 AD for the three records. Higher Pb concentrations recorded in the stalagmite cores (S1, S2 and S3) are observed at depths corresponding in each stalagmite to the periods from ~1880 to 1905 AD and from 1945 to 1965 AD, and a third Pb peak is found around 1980 AD in cores S1 and S2. The Pb values decrease toward the surface of S1 and S2 after 1980 and after 1995 AD for S3. Aluminum concentrations display more variability between cores than the Pb (Fig. 3). In the lower part of S1 and S3 (from 1740 to 1780 AD) the Al concentrations averaged around 5.6 µg g^{-1} for S1 and 56 µg g^{-1} for S3. Higher concentrations of Al in both stalagmites (S1 and S2) occurred in three periods, around 1890 AD, from 1930 to 1940 AD and around 1980 AD. For S3, the Al concentrations display the highest variability from 1870 to 1920 AD.

3.3. Lead isotope ratios

The Pb isotope ratios analyzed in core S1 are displayed in Table 2. In S1, $^{208}Pb/^{206}Pb$ and $^{206}Pb/^{207}Pb$ ranges between 2.150 and 2.072 and from 1.191 to 1.108, respectively. Our data plot well on a straight line

Table 1
Mass-spectrometric U–Th age data for speleothems from Han-Sur Lesse-Cave. Decay constants used to calculate activity ratios from measured atomic ratios are as follows; $\lambda\ ^{238}U = 1.551 * 10^{-10}$. $\lambda\ ^{234}U = 2.835 * 10^{-6}$. $\lambda\ ^{230}Th = 9.915 * 10^{-6}$. $\lambda\ ^{232}Th = 4.948 * 10^{-11}$. Age uncertainties are reported at the 2 σ level. The U–Th age data for S2 is given in Verheyden et al. (2006) and Van Rampelbergh et al. (2014).

Core	mm from top	^{238}U (ppb)	$^{230}Th/^{232}Th$	^{230}Th Age (yr) (uncorrected)	^{230}Th Age (yr) (corrected)	Age (AD)
S1	105	67.8	0.78	571 ± 20	328 ± 13	1682
	630	66.8	4.98	615 ± 17	574 ± 17	1436
	660	52.1	1.96	709 ± 22	590 ± 18	1420
	845	63.8	4.70	822 ± 32	764 ± 29	1246
	1045	73.0	3.15	915 ± 31	820 ± 27	1190
	1215	64.5	3.13	1063 ± 27	952 ± 22	1058
	1400	62.4	3.27	1184 ± 25	1065 ± 22	945
	1520	65.7	3.08	1335 ± 27	1193 ± 24	817
	1677	63.3	4.98	1541 ± 29	1440 ± 29	570
	1850	63.0	60.10	1953 ± 236	1800 ± 35	210
S2	12	154.2	5.2	164 ± 8	30 ± 70	1970
	60	118.6	9.8	194 ± 7	107 ± 44	1893
	112	52.4	20	275 ± 13	215 ± 45	1798
	130	42.9	36	288 ± 17	253 ± 30	1760
	195	41.4	20	435 ± 17	337 ± 71	1676
	250	42.6	44.3	408 ± 17	367 ± 30	1633
	285	57.2	41.3	430 ± 18	384 ± 30	1616
	505	46.7	185	439 ± 23	428 ± 24	1572
	525	52.3	184	459 ± 18	448 ± 19	1552
	545	52.6	188	481 ± 18	470 ± 19	1530
	565	47.5	219	515 ± 22	505 ± 23	1495
	585	41.2	90	570 ± 20	540 ± 25	1460
	1120	54.4	252	870 ± 20	860 ± 23	1140
	1860	65.1	60.7	1947 ± 23	1800 ± 75	200
S3	2	222.1	5.92	36 ± 4	9 ± 14	1995
	32	95.4	70.94	201 ± 17	189 ± 19	1815
	63	129.5	399.13	898 ± 32	888 ± 32	1116
	115	106.0	118.49	1665 ± 35	1604 ± 47	400
	187	123.4	150.64	3159 ± 32	3068 ± 55	−1064
	285	110.7	150.98	5537 ± 49	5380 ± 93	−3376

in a $^{208}Pb/^{206}Pb$ vs $^{06}Pb/^{207}Pb$ diagram (Fig. 5). This means that the data vary between the isotope field defined by the natural sources (Upper Continental Crust and Belgian pre-industrial background) (Sonke et al., 2002; Millot et al. 2004) in the 18th century and the anthropogenic sources in the 20th century defined by the Belgian Zn-smelter (Sonke et al., 2002, 2008), Benelux urban aerosols (Bollhöfer and Rosman, 2001), and the Netherlands gasoline (Hopper et al., 1991).

4. Discussion

4.1. Lead mobilization from soils to speleothems

Recent studies highlight the importance of both organic and inorganic colloidal material for transporting heavy metal from soil to cave (e.g., Borsato et al., 2007; Fairchild et al., 2010; Hartland et al., 2012). The mobility of trace elements is mainly influenced by the soil characteristics and processes (e.g., pH, organic acid content, redox conditions, leaching, ion exchange, temperature). Metals can be transported along the soil profile by colloids or in dissolved forms depending on the metal element (Citeau et al. 2003; Zhao et al. 2009). Several researchers have suggested that organic matter in dissolved or particulate form plays an important role in controlling Pb mobility in the soil (e.g., Kaste et al., 2003; Schwab et al., 2005). The Pb might show different forms of mobility (in dissolved and particulate form) and speeds of migration in soils, depending on soil pH and on the nature of the Dissolved Organic Carbon (DOC) present in the percolating water (Temminghoff et al., 1998; Strobel et al., 2001; Gangloff et al., 2014).

Few studies have investigated the migration of Pb from forest soil to cave (e.g., Borsato et al., 2007; Fairchild et al., 2010; Baldini et al., 2012; Hartland et al., 2012). They suggested that an increased transport of Pb to the speleothem can be attributed to a combination of the effects of a higher presence of mobile organic matter and higher water flow from the soil to the speleothem during periods of more intense rainfall. They further suggested that when Pb is principally transported by organic colloids, this would be indicated by covariation of elements that are strongly bound to colloids (such as Pb and Al). In this study, there is no significant covariation between Pb and Al ($0.04 < r > 0.3$, $0.002 < R^2 > 0.08$) in the 3 available records that would suggest any colloidal transport (Fig. 3). In the absence of covariation between Pb and Al, even if part of the Pb and Al was transported as organic matter metal complexes an important part seems to have been transported in a form bound to inorganic particles. The transfer of Pb signals from the forest soil to the speleothem requires further investigation, but is beyond the scope of the present study.

4.2. Lead content in S1, S2 and S3 speleothem cores

Lead concentrations of the last 250 years in the stalagmite cores S1 and S2 display similar changes with similar timing (Fig. 4). The lead content of stalagmite S3 is ~ten times less than in S1 and S2. This

Table 2
Pb isotopic ratios measured in S1 by MC-ICP-MS Nu Plasma and standard deviations.

Depth from top (cm)	Age max AD	Age min AD	$^{208}Pb/^{206}Pb$	2SE	$^{206}Pb/^{207}Pb$	2SE	Mean Pb concentration (μg g^{-1})
0–0.5	2010	1997	2.098	0.000049	1.162	0.000023	0.15
0.5–0.7	1997	1991	2.105	0.000034	1.154	0.000011	0.34
0.7–0.9	1991	1986	2.102	0.000035	1.157	0.000012	0.58
1–1.4	1983	1973	2.098	0.000036	1.161	0.000011	3.10
1.4–1.6	1973	1968	2.126	0.000036	1.138	0.000014	0.17
1.7–2.2	1966	1955	2.150	0.000032	1.108	0.000012	0.90
2.2–2.5	1955	1950	2.097	0.000042	1.156	0.000016	0.93
2.5–2.8	1950	1946	2.109	0.000094	1.153	0.000038	0.40
2.8–3.4	1946	1938	2.111	0.00036	1.150	0.00010	0.15
3.5–3.9	1937	1932	2.102	0.000066	1.162	0.000028	0.10
5.8–6.5	1907	1897	2.110	0.000060	1.152	0.000023	0.47
7.1–7.8	1887	1878	2.124	0.000033	1.139	0.000009	0.26
7.8–8.8	1787	1776	2.093	0.000029	1.172	0.000012	3.57
8.7–9	1775	1773	2.091	0.000038	1.174	0.000011	0.20
9.1–10	1772	1764	2.084	0.000041	1.180	0.000019	0.12
10–10.4	1764	1760	2.072	0.000035	1.191	0.000018	0.03
10.4–10.9	1760	1755	2.087	0.000037	1.178	0.000013	0.03
10.9–11.2	1755	1753	2.087	0.000052	1.177	0.000024	0.04
11.2–11.8	1753	1747	2.089	0.000060	1.1751	0.000035	0.04

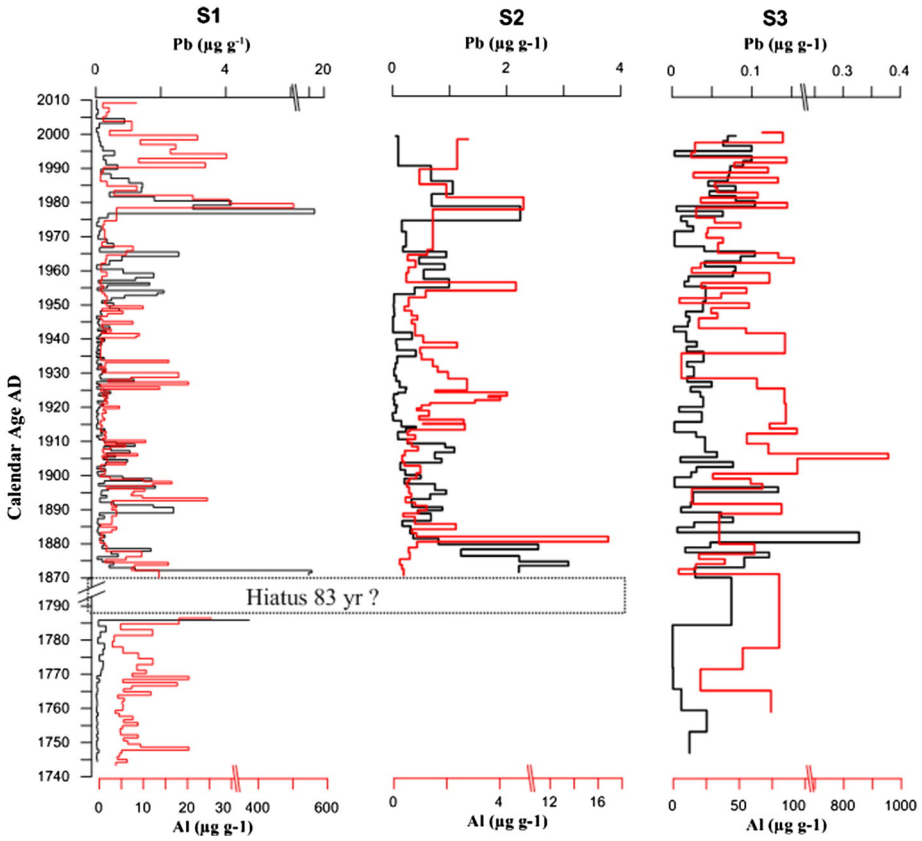

Fig. 3. Pb and Al concentrations (µg g^{-1}) vs age in S1, S2 and S3 stalagmites.

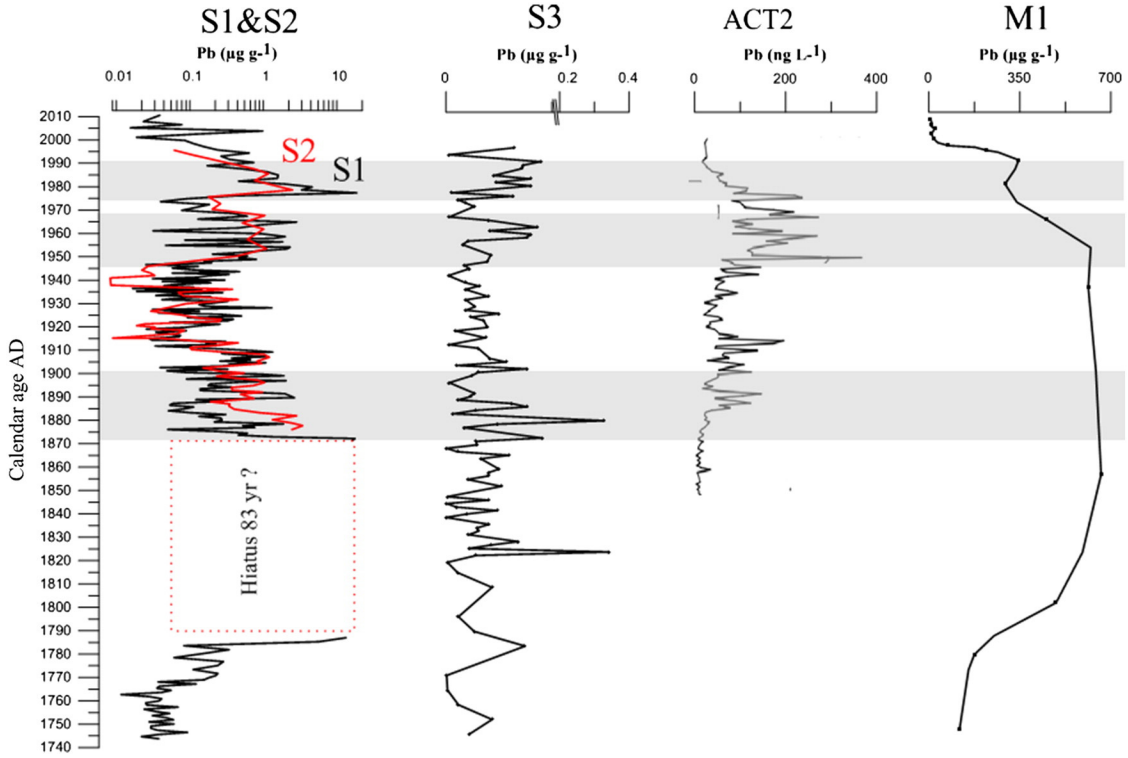

Fig. 4. The correlation of Pb concentration profiles recorded from the three stalagmite cores (S1, S2 and S3), Misten peat bog core (M1) from Belgium (Allan et al., 2013), and ice core (ACT2) from Greenland (McConnell et al., 2006). The three light-gray bars show the maximum concentrations of Pb.

difference in Pb content between S1/S2 and S3 may be attributed to possible differences in chemical composition (Pb/Ca ratio and saturation state) of the initial seepage water in the Salle du Dôme and in the "Réseau renversé" respectively. Chemical monitoring of both dripping places would give more information on the initial state of the water. Unfortunately the Timide (S3) dripping site is extremely slowl nowadays and sampling of sufficient water for a chemical measurement has failed until now. High spatial variability in trace elemental composition of seepage waters in the cave system of Han-sur-Lesse was demonstrated for Mg and Sr in Verheyden et al. (2008). Other studies showed that stalagmites from a same cave may exhibit different trace element patterns (Roberts et al., 1999 and Finch et al., 2003, Baldini et al., 2006), suggesting that different drip sites preserve distinct components of the climate signal. Therefore, a more comprehensive characterization of the spatial hydrochemical variability of several drips from the same cave is essential to understand the causes for observed differences in stalagmite trace element records. The two stalagmites, Proserpine (S1 and S2) and Timide (S3) have different settings and are fed by different hydrological fissure systems. The Proserpine stalagmite is continuously fed by highly saturated seepage water (Van Rampelbergh et al., 2014) and the presented upper 10 cm grew with a rather high rate of ~0.6 mm/year (Verheyden et al., 2006; Van Rampelbergh et al., 2014). The Timide stalagmite (S3) is fed by a slow drip, and grew at 0.17 mm/year. The difference in Pb values between S1–S2 and S3 is most probably due to differences in the hydrological feeding system and residence time of the seepage water. However, the changes observed in S33 over the last 200 years seem to roughly follow the changes observed in the Proserpine stalagmite (S1 and S2 cores) with the occurrence of three periods of higher lead content. The three intervals characterized by particularly high enrichment of Pb were: from 1880 to 1905 AD, from 1945 to 1965 AD, and from 1975 to 1990 AD. The similar timing of occurrence of higher Pb content in cores S1 and S2 of the Proserpine stalagmite and in the S3 stalagmite, despite very different hydrologies and locations, demonstrates the robustness of the Pb signal in a single speleothem and suggests a reproducible Pb variability, but not necessarily Pb amount, in different speleothems from the same cave.

Much lower Pb values are observed before 1760 AD in S1 and are interpreted as background values from a pristine environment compared to the higher lead values after 1760 AD. Early visitors using torches entered the Salle du Dôme since at least ~1700 AD (Timperman, 1989, Verheyden et al., 2006) as indicated by the deposition of gray to brown calcite, but the ash from the torches likely did not affect significantly the Pb record during this period. The S3 stalagmite is located in another part of the cave, cut off by a siphon, preventing direct massive air exchange between both parts. If air-transported aerosols were at the origin of the lead changes in the stalagmites, the Proserpine would have lower Pb content than Timide because Proserpine is continuously washed by dripwater while Timide is relatively 'dry' with long periods between two drips (slow growth) which would enable more aerosols to accumulate on the stalagmite. The reproducibility of lead changes between the two stalagmites, despite being completely different 'local systems' and with different exposure to possible direct anthropogenic contamination suggests the seepage water as the main sources of the Pb in the stalagmite.

Speleothems display Pb enrichments (from 1880 to 1905 AD, from 1945 to 1965 AD, and from 1975 to 1990 AD) seem to roughly track atmospheric lead deposition curves as documented in other archives (Fig. 4). Lead content in a nearby peat bog reconstructed using a core (the Misten bog core, Allan et al., 2013) displays high Pb concentrations from 1770 to 1990 AD. The Misten peat bog is an ombrotrophic peat, i.e. it receives input directly from the atmosphere. Therefore, the recent additional Pb, found in the peat core was of atmospheric origin. This lead was demonstrated in Allan et al. (2013) to have anthropogenic sources. Because of the important difference in chronological resolution of the Pb values in the Misten peat bog and the studied stalagmites it is difficult to compare the two records. However, the fact that higher Pb values are found in the Misten peat between 1770 and 1990, demonstrates that Belgian soils received indeed more lead of anthropogenic origin during these years. Despite the different sampling resolution, the correlation between Pb concentrations in stalagmite cores (S1 and S2) and peat core (M1) is significant. Greenland ice (ice core ACT2) shows an increase in Pb between 1880 and 1915 AD, a higher amount between 1950 and 1970 and a decrease since the 1980s (Fig. 4; McConnell et al., 2006). Likewise a marine record from the *sclerosponge Ceratoporella nicholsoni* (Lazareth et al., 2000) showed a Pb concentration increase occurring between 1840 and 1920 AD and between 1950 and 1990 AD and associated with the global anthropogenic Pb fall-out. The similarity of the global atmospheric lead curves in continental (peat, ice) and marine archives and the speleothem Pb-curves suggests that speleothems recorded at least partly the global anthropogenic atmospheric Pb fall-out. We conclude that Pb concentrations recorded in the S1, S2 and S3 cores may reflect human activities and consequent pollution over the last 250 years.

4.3. The origin of the lead in the stalagmites

Several studies highlight the possible sources of metal content in speleothems, such as the chemical dissolution and mobilization of elements in the soil (Blaser et al., 2000; Jo et al., 2010), or from the surrounding limestone, and aerosol deposition on the stalagmite surface (Dredge et al., 2013). Cave aerosols are sourced from both natural and anthropogenic processes. Aerosol deposition within the cave may also influence speleothem chemistry and may have contributed significantly to speleothem trace element concentrations at some sites (Fairchild et al., 2010). However, Dredge et al. (2013) showed that the aerosol deposition contributions to speleothem surfaces may not be sufficient to influence the speleothem chemistry in many cases. Among the 3 studied speleothem cores, S3 is more exposed to aerosols (open cave) but it contains the lower amount of Pb. The trace metal content in our speleothems is not affected by cave aerosols and more likely reflects the natural and anthropogenic metal coming from surrounding soil layers.

Lead isotope ratios are powerful tools to distinguish between natural atmospheric Pb (supplied primarily by soil dust) and Pb from anthropogenic sources (mining, metallurgical activities, and coal burning). $^{206}Pb/^{207}Pb$ ratios are frequently used in environmental studies to track lead pollution (e.g., Bollhöfer and Rosman, 2001; Shotyk et al., 2000; Weiss et al., 1999). Natural sources of Pb over north-western Europe have $^{206}Pb/^{207}Pb$ ratios that vary between 1.19 and 1.21 (Shotyk et al., 2005; Weis et al., 2005). In the 20th century a significant shift in $^{207}Pb/^{206}Pb$ values was detected in European dust reflecting the strong contribution from anthropogenic sources (Pacyna and Pacyna, 2001; Pacyna et al., 2007). The largest emission of Pb during human history clearly occurred during the 20th century and especially between the 1950s and the 1980s, and is very clearly expressed in archives of past Pb pollution (e.g., Sonke et al., 2002; Shotyk et al., 2005 Cloquet et al., 2006).

Before 1800, all samples in S1 have a $^{206}Pb/^{207}Pb$ ratio higher than 1.172. After 1880, the samples have ratios below 1.162 indicating an increased anthropogenic origin of the lead. This variety of isotopic signatures allows the researchers to distinguish the relative impact of different sources on Pb input from a specific local or regional area. To constrain the anthropogenic sources a binary diagram based on $^{208}Pb/^{206}Pb$ and $^{206}Pb/^{207}Pb$ ratios was used (Fig. 5). The S1 core data plot between the isotope field defined by the Upper Continental Crust (UCC, Millot et al. 2004), through Belgian coal and ores (Cauet and Herbosh, 1982; Dejonghe, 1998) and finally toward a signature of modern Benelux urban aerosols (Bollhöfer and Rosman, 2001) and Belgian smelters (Sonke et al., 2002, 2008). Lead isotope ratios measured in stalagmite samples dated between 1750 and 1780 AD correspond to the Pb isotopic composition of the Belgian Pb–Zn ores

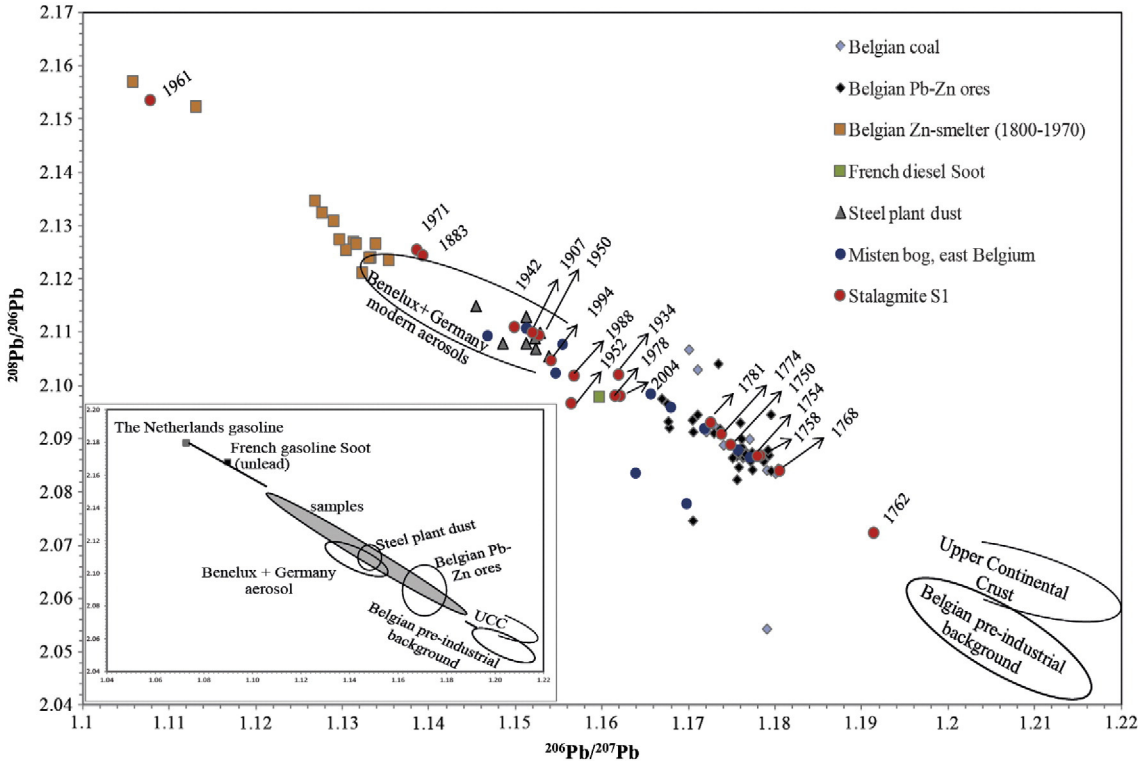

Fig. 5. $^{208}Pb/^{206}Pb$ vs $^{206}Pb/^{207}Pb$ ratios with composition fields of different possible source materials. The age plotted presents the mean age of the interval from which the sample was taken. Stalagmite samples (red dots), Misten bog (blue dots), Upper Continental Crust from Millot et al. (2004), Belgian pre-industrial sediment from Sonke et al. (2002), Belgian coal and ores (blue and black diamond) from Cauet and Herbosh (1982), Dejonghe (1998), Benelux urban aerosols from Bollhöfer and Rosman (2001) and Belgian smelter (orange squares) from Sonke et al. (2008). The signature for steel plant dust (gray triangles — data from Geagea et al., 2007), French diesel and gasoline (green squares — from Geagea et al., 2008), and Netherlands gasoline (Hopper et al., 1991) are plotted for comparison. (For interpretation of the references to color in this figure legend, the reader is referred to the web version of this article.)

(Durali-Mueller et al., 2007) with a minor contribution from the natural sources defined by the Upper Continental Crust (Millot et al. 2004) and Belgian pre-industrial background (Sonke et al., 2002). The samples located between 1880 and 1961 AD have isotope ratios close to the values of the Belgian Zn-smelter, steel plant dust and Benelux aerosols. In 1961 AD, a particularly important decrease in $^{206}Pb/^{207}Pb$ ratios is consistent with an increase in the Belgian smelter contribution and consumption of leaded gasoline inset (Fig. 5). This sample has the isotope ratios nearest to the values of the Belgian Zn-smelter and Netherlands gasoline (Hopper et al., 1991), which reflected the impact of leaded gasoline used in Europe. This observation agrees with the observation of Von Storch et al. (2003), who proposed that Pb from gasoline was the dominant anthropogenic source of Pb in 1965 AD. The use of leaded gasoline increased from 1930 to a maximum in the 1970s. The progressive reduction of lead in gasoline started in 1972 (Von Storch et al., 2003).

The samples located in the upper part of the stalagmite (1970–2004 AD) have isotope ratios close to the Belgian Zn-smelter and the modern aerosols collected above Benelux and Germany. Our results are consistent with previous data recorded in the Misten peat bog core (Allan et al., 2013 — Fig. 5). In Misten core (M1), $^{206}Pb/^{207}Pb$ ratios decreased from 1.175 to 1.155 (between 1748 and 1953 AD) corresponding to the isotopic fields representing Belgian coal and Pb–Zn ores. The sample located in the upper part of the Misten core (1969–1977) has isotope ratios nearest to the values of the Belgian Zn-smelter and Benelux aerosols. The youngest samples (from 1994 to 2007 AD) are characterized by an increase in isotopic ratios $^{206}Pb/^{207}Pb$ ratios (from 1.151 to 1.169). This increase is linked to the increased Belgian smelter and refinery activity during that period. The Pb isotope ratios of this study strongly suggest that the Han-sur-Lesse stalagmites are influenced by a mixture of local and regional anthropogenic Pb sources, and track increases in anthropogenic Pb pollution through time.

4.4. Human activity and Pb atmospheric pollution records

Following the advent of the Industrial Revolution in the mid-1700s, anthropogenic emissions of trace elements (e.g., Pb) to the atmosphere largely dominated the natural inputs (e.g., Nriagu, 1989). Trace metal concentrations in the Han-sur-Lesse cave stalagmites increase markedly in calcite deposited after 1880 AD, and this increase is indirectly attributable to increased anthropogenic trace element emissions at both regional and global scales. These Pb/Al profiles are similar to those observed in the Misten peat bog core (Fig. 6; Allan et al., 2013).

Around 1770 AD, the Pb/Al values in S1 begin to increase, synchronous with a decrease in $^{206}Pb/^{207}Pb$ ratios, and reach high values between 1770 and 1790 AD. This trend is attributable to the Industrial Revolution (Fig. 6). From 1880 to 1907 AD, the $^{206}Pb/^{207}Pb$ ratio shows lower values ($^{206}Pb/^{207}Pb$ up to 1.139 at 1883 and to 1.152 at 1907 AD) reflecting an increase in Pb/Al values in all stalagmite cores, which is probably the result of the inception of the Belgian metal industry (Pb at around 1830) (Schmitz, 1979; Dejonghe, 1998). Coal production started in Belgium in 1830 AD (Rutledge, 2011) and increased significantly to reach its maximum (~30 million metric tons yr^{-1}) between 1927 and 1955 AD. During WWI and WWII, the cave was closed, explaining the whiter calcite deposited around 1917 AD and between 1940 and 1945 AD (Fig. 2).

Since 1945 AD, $^{206}Pb/^{207}Pb$ ratios drop toward 1.107 (1961 AD) reflecting increasing gasoline Pb contributions. The maximum Pb/Al values (between 1945 and 1990 AD) reflect peak Belgian smelter and refinery activity (Schmitz, 1979; USGS). The maximum anthropogenic emissions of Pb occurred between 1955 and 1990 AD (Fig. 6 — Nriagu,

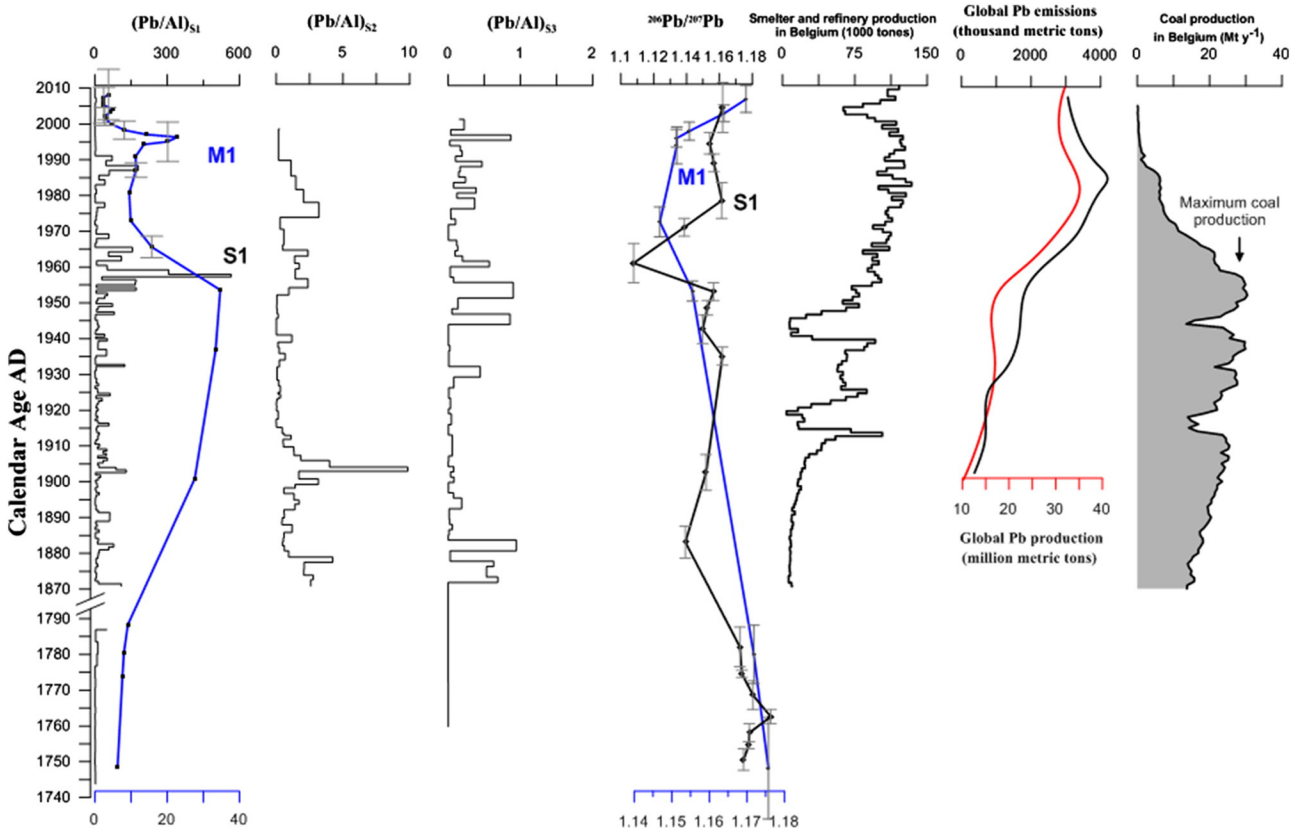

Fig. 6. Comparison between the Pb/Al ratio in all stalagmite cores and M1 peat core, Pb isotopic record in S1 and M1 with the Belgian production of coal (Rutledge, 2011), smelter and refinery production (Pb) in Belgium (Rutledge, 2011), and with global production and emissions of Pb (Nriagu, 1996; USGS).

1996) and varied between 3600 and 4800 metric tons per year (p.a.) in Belgium (Von Storch et al., 2003), while coal consumption was at its maximum in Europe. This substantial increase in atmospheric pollution is recorded in Han-sur-Lesse stalagmites as increased Pb/Al values, associated with a small decrease of $^{206}Pb/^{207}Pb$ ratio (1.157).

The samples located in the upper part of the core S1 (1995–2004) have isotope ratios nearest to the values of the steel plant dust and Benelux aerosols. The Pb/Al values in S1 decrease from 1995 to the date of sampling of 2011, coincident with increasing $^{206}Pb/^{207}Pb$ ratios, consistent with results obtained from Misten bog (Allan et al., 2013). This reduction in trace element pollution reflects progressive phasing out of coal combustion in Belgium, decreases in global emission of heavy metals and also results from the disappearance of leaded gasoline. However, despite the reduction of atmospheric pollution during recent years, the dominant sources of trace metals measured in our stalagmites remain anthropogenic.

5. Conclusion

High resolution records of Pb concentrations coupled with Pb isotope ratios from the Han-sur-Lesse cave stalagmites in southern Belgium provide a record of changing inputs of trace elements to the region over the last 250 years. The geochemical results presented here recorded natural processes prior to the Industrial Revolution, but have since predominantly reflected shifting sources of anthropogenic pollution. Intervals characterized by Pb enrichment exist in the speleothems and represent the intervals from 1880 to 1905 AD, from 1945 to 1965 AD, and from 1975 to 1990 AD. Lead isotope ratios indicate diverse sources of atmospheric contamination (coal, industrial, steel production, road dust) which change through time. The history of Pb pollution revealed by both Han-sur-Lesse speleothems shows some agreement with other Pb records, and clearly reflects the increasing influence of atmospheric metal pollution since the advent of the Industrial Revolution. These changes confirm that stalagmites are sensitive to external anthropogenic atmospheric pollution. This paper therefore highlights their potential as an alternative archive in continental settings to reconstruct atmospheric contamination, e.g., pollution, volcanic fall-out, dust deposits, with an accurate time frame based on independent chronological tracers (U/Th, ^{14}C, and lamination). This research underscores the importance of speleothems as a valuable tool for the discrimination between anthropogenic and natural lead contributions in the environment and consequently for quantifying the anthropogenic contribution or determining natural background values.

Supplementary data to this article can be found online at http://dx.doi.org/10.1016/j.chemgeo.2015.02.035.

Acknowledgments

We thank all the persons who contribute to this work and especially Jacque Navez, Laurence Monin from (LA-ICP-MS analyses), Nadine Mattielli and Ivan Petrov at ULB (MC-ICP-MS analyses), and Dr Chris Ottley at Durham (ICP-MS analyses). This study was funded by the Walloon Region (Visa 08/13701) and the FNRS. M. Allan received funding through a PhD grant from the government of Syria and Erasmus Mundus EPIC. Thanks to the personal of Han-sur-Lesse caves and especially to Mme. Malou, Guy Evrard and the guide Etienne Lannoye for their help during sampling. The manuscript has been improved by the constructive comments of the reviewers and by the editor, Dr. L Reisberg.

References

Allan, M., Le Roux, G., De Vleeschouwer, F., Mattielli, N., Piotrowska, N., Sikorski, J., Fagel, N., 2013. Reconstructing historical atmospheric mercury deposition in Western Europe using: Misten peat bog cores Belgium. Environ. Pollut. 178, 381–394.

Baker, A., Ito, E., Smart, P.L., McEwan, R.F., 1997. Elevated and variable values of C-13 in speleothems in a British cave system. Chem. Geol. 136, 263–270.

Baldini, J., McDermott, F., Fairchild, I., 2006. Spatial variability in cave drip water hydrochemistry: implications for stalagmite paleoclimate records. Chem. Geol. 235, 390–404.

Baldini, J.U.L., McDermott, F., Baldini, L.M., Ottley, C.J., Linge, K.L., Clipson, N., Jarvis, K.E., 2012. Identifying short-term and seasonal trends in cave drip water trace element concentrations based on a daily-scale automatically collected drip water dataset. Chem. Geol. 330–331, 1–16.

Blaser, P., Zimmermann, S., Luster, J., Shotyk, W., 2000. Critical examination of trace element enrichments and depletion in soils: As, Cr, Cu, Ni Pb and Zn in Swiss forest soils. Sci. Total Environ. 249, 257–280.

Bollhöfer, A., Rosman, K.J.R., 2001. Lead isotopic ratios in European atmospheric aerosols. Phys. Chem. Earth B 26 (10), 835–838.

Bonniver, I., 2011. Etudehydrogéologique et dimensionnement par modélisation du sytème-traçage du réseaukarstique de Han-sur-Lesse (Massif de Boine — Belgique). Faculté des Sciences, Département de Géologie, Faculté Notre-Dame de Namur (FUNDP), unpublished PhD thesis. 349p.

Borsato, A., Frisia, S., Fairchild, I.J., Somogyi, A., Susini, J., 2007. Trace element distribution in annual stalagmite laminae mapped by micrometer-resolution X-ray fluorescence: implications for incorporation of environmentally significant species. Geochim. Cosmochim. Acta 71, 1494–1512.

Boutron, C.F., Görlach, U., Candelone, J.P., Bolshov, M.A., Delmas, R.J., 1991. Decrease in anthropogenic lead, cadmium and zinc in Greenland snows since the late 1960s. Nature 353, 153–156.

Boutron, C.F., Candelone, J.P., Hong, S., 1994. Past and recent changes in the large scale tropospheric cycles of lead and other heavy metals as documented in Antarctic and Greenland snow and ice: a review. Geochim. Cosmochim. Acta 58, 3217–3225.

Brännvall, M.-L., Bindler, R., Renberg, I., Emteryd, O., Bartnicki, J., Billström, K., 1999. The medieval metal industry was the cradle of modern large-scale atmospheric lead pollution in northern Europe. Environ. Sci. Technol. 33, 4391–4395.

Cauet, S.W.D., Herbosh, A., 1982. Genetic study of Belgian lead zinc mineralizations in carbonate environments through lead isotope geochemistry. Bull. BRGM 3, 29–41.

Chang, S.J., Jeong, G.Y., Kim, S.J., 2008. The origin of black carbon on speleothems in tourist caves in South Korea: chemical characterization and source discrimination by radiocarbon measurement. Atmos. Environ. 42, 1790–1800.

Cheng, H., Edwards, R.L., Broecker, W.S., Denton, G.H., Kong, X., Wang, Y., Zhang, R., Wang, X., 2009a. Ice age terminations. Science 326, 248–252.

Cheng, H., Fleitmann, D., Edwards, R.L., Wang, X.F., Cruz, F.W., Auler, A.S., Mangini, A., Wang, Y.J., Kong, X.G., Burns, S.J., Matter, A., 2009b. Timing and structure of the 8.2 kyr BP event inferred from delta O-18 records of stalagmites from China, Oman, and Brazil. Geology 37, 1007–1010.

Citeau, L., Lamy, I., van Oort, F., Elsass, F., 2003. Colloidal facilitated transfer of metals in soils under different land use. Colloids Surf. A Physicochem. Eng. Asp. 217, 11–19.

Cloquet, C., Carignan, J., Libourel, G., 2006. Atmospheric pollutant dispersion around an urban area using trace metal concentrations and Pb isotopic compositions in epiphytic lichens. Atmos. Environ. 40 (3), 574–587.

Dejonghe, L., 1998. Zinc–lead deposits of Belgium. Ore Geol. Rev. 12, 329–354.

Dredge, J., Fairchild, I.J., Harrison, R.M., Fernandez-Cortes, A., Sanchez-Moral, S., Jurado, V., Gunn, J., Smith, A., Spoetl, C., Mattey, D., Wynn, P.M., Nathalie, G., 2013. Cave aerosols: distribution and contribution to speleothem geochemistry. Quatern. Sci. Rev. 63, 23–41.

Drysdale, R.N., Hellstrom, J.C., Zanchetta, G., Fallick, A.E., Sanchez Go, M.F., Couchoud, I., McDonald, J., Maas, R., Lohmann, G., Isola, I., 2009. Evidence for obliquity forcing of glacial termination II. Science 325, 1527–1531.

Durali-mueller, S., Grey, G.P., Wigg-Wolf, D., Lahaye, Y., 2007. Roman lead mining in Germany: its origin and development through time deduced from lead isotope provenance studies. J. Archeol. Sci. 34, 1555–1567.

Edwards, R.L., Chen, J.H., Wasserburg, G.J., 1987. ^{238}U–^{234}U–^{230}Th–^{232}Th systematic and the precise measurement of time over the past 500,000 years. Earth Planet. Sci. Lett. 81, 175–192.

Elless, M.P., Lee, S.Y., 1998. Uranium solubility of carbonate-rich uranium-contaminated soils. Water Air Soil Pollut. 107, 147–162.

Fairchild, I.J., Baker, A., 2012. Speleothem Science. From Process to Past Environments. Wiley-Blackwell, Chichester, p. 432.

Fairchild, I.J., Treble, P.C., 2009. Trace elements in speleothems as recorders of environmental change. Quatern. Sci. Rev. 28 (5–6), 449–468.

Fairchild, I.J., Baker, A., Borsato, A., Frisia, S., Hinton, R.W., McDermott, F., Tooth, A.F., 2001. Annual to sub-annual resolution of multiple trace-element trends in speleothems. J. Geol. Soc. 158 (5), 831–841.

Fairchild, I.J., Spötl, C., Frisia, C., Borsato, A., Susini, J., Wynn, P.M., Cauzid, J., EIMF, 2010. Petrology and geochemistry of annually laminated stalagmites from an Alpine cave (Obir, Austria): seasonal cave physiology. Geol. Soc. Lond. Spec. Publ. 336, 295–321.

Finch, A., Shaw, P., Holmgren, K., Lee-Thorp, J., 2003. Corroborated rainfall records from aragonitic stalagmites. Earth Planet. Sci. Lett. 215, 265–273.

Fleitmann, D., Borsato, A., Frisia, S., Badertscher, S., Cheng, H., REdwards, L., Tüysüz, O., 2012. Speleothems as sensitive recorders of volcanic eruptions — the Bronze Age Minoan eruption recorded in a stalagmite from Turkey. EGU General Assembly 2012, Held 22–27 April, 2012 in Vienna, Austria.

Frisia, S., Borsato, A., Fairchild, I.J., Susini, J., 2005. Variations in atmospheric sulphate recorded in stalagmites by synchrotron micro-XRF and XANES analyses. Earth Planet. Sci. Lett. 235, 729–740.

Gangloff, S., Stille, P., Pierette, M.C., Weber, T., Chabaux, F., 2014. Characterization and evolution of dissolved organic matter in acidic forest soil and its impact on the mobility of major and trace elements (case of the Strengbach watershed). Geochim. Cosmochim. Acta 130, 21–41.

Geagea, M.L., Stille, P., Millet, M., Perrone, T., 2007. REE characteristics and Pb, Sr and Nd isotopic compositions of steel plant emissions. Sci. Total Environ. 373, 404–419.

Geagea, M.L., Stille, P., Gauthier-Lafaye, F., Millet, M., 2008. Tracing of industrial aerosol sources in an urban environment using Pb, Sr, and Nd isotopes. Environ. Sci. Technol. 42, 692–698.

Genty, D., Massault, M., 1999. Carbon transfer dynamics from bomb-14C and d13C time series of a laminated stalagmite from SW-France–modelling and comparison with other stalagmite. Geochim. Cosmochim. Acta 63, 1537–1548.

Genty, D., Blamart, D., Ouahdi, R., Gilmour, M., Baker, A., Jouzel, J., Van- Exter, S., 2003. Precise dating of Dansgaard–Oeschger climate oscillations in western Europe from stalagmite data. Nature 421, 833–837.

Genty, D., Blamart, D., Ghaleb, B., Plagnes, V., Causse, C.h., Bakalowicz, M., Zouari, K., Chkir, N., Hellstrom, J., Wainer, K., Bourges, F., 2006. Timing and dynamics of the last deglaciation from European and North African d13C stalagmite profiles—comparison with Chinese and South Hemisphere stalagmites. Quatern. Sci. Rev. 25, 2118–2142.

Gobeil, C., Macdonald, R.W., Smith, J.N., 1999. Mercury profiles in sediments of the Arctic Ocean basins. Environ. Sci. Technol. 33, 4194–4198.

Hartland, A., Fairchild, I.J., Lead, J.R., Zhang, H., Baalousha, M., 2011. Size, speciation and lability of NOM-metal complexes in hyper alkaline cave dripwater. Geochim. Cosmochim. Acta 75, 7533–7551.

Hartland, A., Fairchild, I.J., Lead, J.R., Borsato, A., Baker, A., Frisia, S., Baalousha, M., 2012. From soil to cave: transport of trace metals by natural organic matter in dripwaters. Chem. Geol. 304, 68–82.

Hellstrom, J., McCulloch, M., Stone, J., 1998. A detailed 31,000 year record of climate and vegetation change, from the isotope geochemistry of two New Zealand speleothems. Quatern. Sci. 50, 167–178.

Hong, S.M., Candelone, J.P., Patterson, C.C., Boutron, C.F., 1994. Greenland ice evidence of hemispheric lead pollution two millennia ago by Greek and Roman civilizations. Science 265, 1841–1843.

Hopper, J.F., Ross, H.B., Sturges, W.T., Barrie, L.A., 1991. Regional source discrimination of atmospheric aerosols in Europe using the isotopic composition of lead. Tellus 43B, 45–60.

Jo, K.N., Woo, K.S., Hong, G.H., Kim, S.H., Suk, B.C., 2010. Rainfall and hydrological controls on speleothem geochemistry during climatic events (droughts and typhoons): an example from Seopdong Cave, Republic of Korea. Earth Planet. Sci. Lett. 295 (3–4), 441–450.

Kaste, J.M., Friedland, A.J., Stürup, S., 2003. Using stable and radioactive isotopes to trace atmospherically deposited Pb in Montane forest soils. Environ. Sci. Technol. 37, 2567–3560.

Kaufman, A., Wasserburg, G.J., Porcelli, D., Bar-Matthews, M., Ayalon, A., Halicz, L., 1998. U–Thisotope systematics from the Soreq Cave, Israel, and climatic correlations. Earth Planet. Sci. Lett. 156, 141–155.

Lazareth, C.E., Willenz, P., Navez, J., Keppens, E., Dehairs, F., André, L., 2000. Sclerosponges as a new potential recorder of environmental changes: lead in *Ceratoporella nicholsoni*. Geology 28 (6), 515–518.

Li, W.X., Lundberg, J., Dickin, A.P., Ford, D.C., Schwarcz, H.P., McNutt, R.H., Williams, D., 1989. High-precision mass-spectrometric uranium-series dating of cave deposits and implications for palaeoclimate studies. Nature 339–534.

Mangini, A., Spötl, C., Verdes, P., 2005. Reconstruction of temperature in the Central Alps during the past 2000 yr from a delta O18 stalagmite record. Earth Planet. Sci. Lett. 235, 741–751.

Mattey, D., et al., 2008. A 53 year seasonally resolved oxygen and carbon isotope record from a modem Gibraltar speleothem: reconstructed drip water and relationship to local precipitation. Earth Planet. Sci. Lett. 269, 80–95.

McConnell, J.R., Kipfstuhl, S., Fischer, H., 2006. The NGT and PARCA shallow ice core arrays in Greenland: a brief overview. PAGES News 14 (1), 13–14.

McDermott, F., Atkinson, T.C., Fairchild, I.J., Baldini, L.M., Mattey, D.P., 2011. A first evaluation of the spatial gradients in d18O recorded by European Holocene speleothems. Global Planet. Chang. 79, 275–287.

McFarlane, D.A., Lundberg, J., Neff, H., 2013. A speleothem record of Early British and Roman Mining at Charterhouse, Mendip England. Archaeometry 2013. http://dx.doi.org/10.1111/arcm.12025.

McMillan, E.A., Fairchild, I.J., Frisia, S., Borsato, A., McDermott, F., 2005. Annual trace element cycles in calcite-aragonite speleothems: evidence of drought in the western Mediterranean 1200–1100 yr BP. J. Quatern. Sci. 20, 423–433.

Millot, R., Allègre, C.J., Gaillardet, J., Roy, S., 2004. Lead isotopic systematics of major river sediments: a new estimate of the Pb isotopic composition of the Upper Continental Crust. Chem. Geol. 203, 75–90.

Nriagu, J.O., 1979. Global inventory of natural and anthropogenic emissions of trace metals to the atmosphere. Nature 279, 409–411.

Nriagu, J.O., 1989. A global assessment of natural sources of atmospheric trace metals. Nature 338, 47–49.

Nriagu, J.O., 1996. A history of global metal pollution. Science 272 (5259), 223–224.

Outridge, P.M., Rausch, N., Percival, J.B., Shotyk, W., a McNeely, R., 2011. Comparison of mercury and zinc profiles in peat and lake sediment archives with historical changes in emissions from the FlinFlon metal smelter, Manitoba, Canada. Sci. Total Environ. 409, 548–563.

Pacyna, J.M., Pacyna, E.G., 2001. An assessment of global and regional emissions of trace metals to the atmosphere from anthropogenic sources worldwide. Environ. Rev. 9, 269–298.

Pacyna, E.G., Pacyna, J.M., Fudala, J., Strzelecka-Jastrzab, E., Hlawiczka, S., Panasiuk, D., Nitter, S., Pregger, T., Pfeiffer, H., Friedrich, R., 2007. Current and future emissions of selected heavy metals to the atmosphere from anthropogenic sources in Europe. Atmos. Environ. 41, 8557–8566.

Quinif, Y., Bastin, B., 1986. Le systéme karstique de Han-sur-Lesse (Belgique). Actes Cong. Int. Espeleol 1. International Congressof Speleology, Spain, Barcelona, pp. 147–161.
Roberts, M., Smart, P., Hawkesworth, C., Perkins, W., Pearce, N., 1999. Trace element variations in coeval Holocene speleothems from GB Cave, southwest England. The Holocene 9, 707–713.
Rosman, K.J.R., Chisholm, W., Hong, S.M., Candelone, J.P., Boutron, C.F., 1997. Lead from Carthaginian and Roman Spanish mines isotopically identified in Greenland ice dated from 600 BC to 300 AD. Environ. Sci. Technol. 31, 3413–3416.
Rutledge, D., 2011. Estimating long-term world coal production with logit and probit transforms. Int. J. Coal Geol. 85, 23–31.
Schmitz, C., 1979. World Non-Ferrous Metal Production and Prices. 1700–1976. Routledge Chapman and Hall.
Scholte, P., De Geest, P., 2010. The climate of Socotra Island (Yemen): a first-time assessment of the timing of the monsoon wind reversal and its influence on precipitation and vegetation patterns. J. Arid Environ. 74, 1507–1515.
Schwab, A.P., Yinghong, H., Banks, M.K., 2005. The influence of organic ligands on the retention of lead in soil. Chemosphere 61, 856–866.
Shirahata, H., Elias, R.W., Patterson, C.C., 1980. Chronological variations in concentrations and isotopic compositions of anthropogenic atmospheric lead in sediments of a remote subalpine pond. Geochim. Cosmochim. Acta 44, 149–162.
Shotyk, W., Blaser, P., Grünig, A., Cheburkin, A.K., 2000. A new approach for quantifying cumulative, anthropogenic, atmospheric lead deposition using peat cores from bogs: Pb in eight Swiss peat bog pro files. Sci. Total Environ. 249 (1–3), 281–295.
Shotyk, W., Goodsite, M.E., Roos-Barraclough, F., Givelet, N., Le Roux, G., Weiss, D., Chemburkin, A.K., Knudden, K., Heinemeier, J., Van Der Knaap, W.O., Norton, S.A., Lohse, C., 2005. Accumulation rates and predominant atmospheric sources of natural and anthropogenic Hg and Pb on the Faroe Islands. Geochim. Cosmochim. Acta 69 (1), 1–17.
Siklosy, Z., Kern, Z., Demeny, A., Pilet, S., Leel-Ossy, S., Lin, K., Shen, C.C., Szeles, E., Breitner, D., 2011. Speleothems and pine trees as sensitive indicators of environmental pollution—a case study of the effect of uranium-ore mining in Hungary. Appl. Geochem. 26, 666–678.
Sonke, J.E., Hoogewerf, J.A., van der Laan, S.R., Vangronsveld, J.A., 2002. Chemical and mineralogical reconstruction of Zn-smelter emissions in the Kempen region (Belgium), based on organic pool sediment cores. Sci. Total Environ. 292, 101–119.
Sonke, J.E., Sivry, Y., Viers, J., Freydier, R., Dejonghe, L., Andre, L., Aggarwal, J.K., Fontan, F., Dupre, B., 2008. Historical variations in the isotopic composition of atmospheric zinc deposition from a zinc smelter. Chem. Geol. 252, 145–157.
Strobel, B.W., Hansen, H.C.B., Borggaard, O.K., Andersen, M.K., Raulund-Rasmussen, K., 2001. Composition and reactivity of DOC in forest floor soil solutions in relation to tree species and soil type. Biogeochemistry 56, 1–26.
Temminghoff, E.J.M., Van der Zee, S.E.A.T.M., De Haan, F.A.M., 1998. Effects of dissolved organic matter on the mobility of copper in a contaminated sandy soil. Eur. J. Soil Sci. 49, 617–628.
Timperman, M., 1989. La Grotte de Han au fil des Siècles. USGS (United States Geological Survey)Ed. Duculot, Gembloux, Belgium (66 pp. http://minerals.usgs.gov/minerals/pubs.).
Van Rampelbergh, M., Verheyden, S., Allan, M., Quinif, Y., Keppens, E., Claeys, P., 2014. Seasonal variations recorded in cave monitoring results and a 10 year monthly resolved speleothem $\delta^{18}O$ and $\delta^{13}C$ record from the Han-sur-Lesse cave, Belgium. Clim. Past Discuss. 10 (1821–1856), 2014. http://dx.doi.org/10.5194/cpd-10-1821-2014.
Verheyden, S., Baele, J.M., Keppens, E., Genty, D., Cattani, O., Cheng, H., Lawrence, E., Zhang, H., Van Strijdonck, M., Quinif, Y., 2006. The Proserpine stalagmite (Han-sur-Lesse Cave, Belgium): preliminary environmental interpretation of the last 1000 years as recorded in a layered speleothem. Geol. Belg. 9 (3–4), 245–256.
Verheyden, S., Nader, F.H., Cheng, H.J., Edwards, L.R., Swennen, R., 2008. Paleoclimate reconstruction in the Levant region from the geochemistry of a Holocene stalagmite from the Jeita Cave. Lebanon Quatern. Res. 70, 368–381.
Von Storch, H., Costa-Cabral, M., Hagner, C., Feser, F., Pacyna, J., Pacyna, E., Kolb, S., 2003. Four decades of gasoline lead emissions and control policies in Europe: a retrospective assessment. Sci. Total Environ. 311 (1–3), 151–176.
Wang, Y.J., Cheng, H., Edwards, L., Kong, X., Shao, X., Chen, S., Wu, J., Jiang, X., wang, X., wang, X., An, Z., 2008. Millennial- and orbital-scale changes in the East Asian monsoon over the past 224,000 years. Nature 451, 1090–1093.
Weis, D., Kieffer, B., Maerschalk, C., Pretorius, W., Barling, J., 2005. High precision Pb–Sr–Nd–Hf isotopic characterization of USGS BHVO-1 and BHVO-2 reference materials: comparison of first and second generation samples. Geochem. Geophys. Geosyst. 6, Q02002. http://dx.doi.org/10.1029/2004GC000852.
Weiss, D.J., Shotyk, W., Schafer, J., Loyall, U., Grollimund, E., Gloor, M., 1999. Microwave digestion of ancient peat and lead determination by voltammetry. Fresenius J. Anal. Chem. 363, 300–305.
Wynn, P.M., Fairchild, I.J., Baker, A., Frisia, S., Borsato, A., Baldini, J., McDermott, F., 2008. Isotopic archives of sulphur in speleothems. Geochim. Cosmochim. Acta 72, 2465–2477.
Wynn, P.M., Fairchild, I.J., Frisia, S., Spotl, C., Baker, A., Borsato, 2010. High-resolution sulphur isotope analysis of speleothem carbonate by secondary ionisation mass spectrometry. Chem. Geol. 271, 101–107.
Wynn, P.M., Fairchild, I.J., Spötl, C., Hartland, A., Mattey, D., Fayard, B., Cotte, M., 2014. Synchrotron X-ray distinction of seasonal hydrological and temperature patterns in speleothem carbonate. Environ. Chem. 11 (1), 28–36.
Zhao, L.Y.L., Schulin, R., Nowack, B., 2009. Cu and Zn mobilization in soil columns percolates by different irrigation solutions. Environ. Pollut. 157, 823–833.